

Realtime Motion Generation with Active Perception Using Attention Mechanism for Cooking Robot

Namiko Saito^{1,2,3}, Mayu Hiramoto¹, Ayuna Kubo¹, Kanata Suzuki^{4,6}, Hiroshi Ito^{5,6},
Shigeki Sugano¹ and Tetsuya Ogata^{6,7}

Abstract—To support humans in their daily lives, robots are required to autonomously learn, adapt to objects and environments, and perform the appropriate actions. We tackled on the task of cooking scrambled eggs using real ingredients, in which the robot needs to perceive the states of the egg and adjust stirring movement in real time, while the egg is heated and the state changes continuously. In previous works, handling changing objects was found to be challenging because sensory information includes dynamical, both important or noisy information, and the modality which should be focused on changes every time, making it difficult to realize both perception and motion generation in real time. We propose a predictive recurrent neural network with an attention mechanism that can weigh the sensor input, distinguishing how important and reliable each modality is, that realize quick and efficient perception and motion generation. The model is trained with learning from the demonstration, and allows the robot to acquire “human-like” skills. We validated the proposed technique using the robot, Dry-AIREC, and with our learning model, it could perform cooking eggs with unknown ingredients. The robot could change the method of stirring and direction depending on the status of the egg, as in the beginning it stirs in the whole pot, then subsequently, after the egg started being heated, it starts flipping and splitting motion targeting specific areas, although we did not explicitly indicate them. See our accompanying video here: <https://youtu.be/PHHMDUO0mHU>

I. INTRODUCTION

There is an increasing demand for robots that work and support daily tasks [1]–[3]. We aim for the realization of an AI robot that autonomously learns, adapts to its environment, evolves, and acts alongside human beings. The robot must recognize the demanded goal, perceive the current situations, and generate motions autonomously. Cooking scenarios, in particular, contain challenging research questions. In our daily lives, we use ingredients with complicated and fragile characteristics, which change and deform continuously due to heat and force; therefore, we must perceive the state of the

*This research has received funding from JSPS Grant-in-Aid for Scientific Research (A) No. 19H01130, JST Moonshot R & D Grant Number JPMJMS2031 and Waseda Research Institute for Science and Engineering.

¹Authors are with Department of Modern Mechanical Engineering, Waseda University, Tokyo, Japan.

²Author is with the School of Informatics, The University of Edinburgh, Edinburgh, U.K. namiko.saito@ed.ac.uk

³Author is with The Alan Turing Institute, London, U.K.

⁴Author is with the Artificial Intelligence Laboratories, Fujitsu Limited, Kanagawa, Japan

⁵Author is with the Center for Technology Innovation - Controls and Robotics, Research & Development Group, Hitachi, Ltd., Ibaraki, Japan

⁶Authors are with the Department of Intermedia Art and Science, Waseda University, Tokyo, Japan.

⁷Author is with the National Institute of Advanced Science and Technology, Tokyo, Japan.



Fig. 1: The humanoid robot, Dry-AIREC, cooks scrambled eggs in a kitchen. Our aim is to support humans’ daily lives with the artificial intelligence robot.

ingredients in real-time. Furthermore, we continuously adopt cooking motions, such as stirring, splitting, and flipping over, depending on the state of the ingredients. In this study, we tackle the questions and develop a robot that can perceive the characteristics of target objects in real time and perform motion accordingly, which has not been achieved before. As an example, we demonstrate a robot cooking scrambled eggs, in which it is required to change the method of stirring and direction depending on the status of the egg.

To handle ingredients flexibly, the robot must recognize not only the extrinsic characteristics but also the intrinsic characteristics [4]–[6]. The extrinsic characteristics are related to appearance, such as shape, color, size, posture, and position. The intrinsic ones include physical characteristics such as weight, friction, and stiffness. Extrinsic characteristics are thus visible, whereas intrinsic ones are not, and are instead perceived through tactile and proprioceptive senses. Several factors for deciding actions depend on both characteristics, such as motion speed, timing, trajectory, and force strength. If robots cannot recognize the extrinsic characteristics, they often fail the cooking tasks; for example, they may burn the ingredients. On the other hand, if they cannot recognize intrinsic characteristics, they also fail; such as they may crush the ingredients and some parts are remained raw. However, several previous studies on cooking robotics have not considered these characteristics in real time, and they combined specific motions fixing parameters like task duration and heating power, and played them as [7], [8]. They realized efficient execution of cooking; however, the process

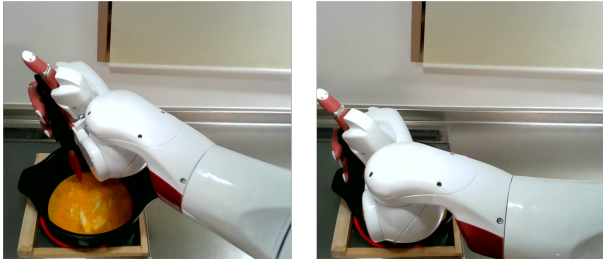


Fig. 2: In the left picture, the robot arm does not touch the pot; thus, tactile and torque sensor information is less important than visual information. In the right picture, the robot occludes the pot with its own arm; thus, the image has less meaning than tactile and torque information.

was not flexible to ingredients status. Some research tackled extrinsic characteristics which change with motions using vision; however, they did not consider intrinsic characteristics [9]–[12]. [13] realized that motion adaptation depends on intrinsic characteristics; however, the characteristics had to be annotated by humans and not recognized by the robot. [14], [15] showed how objects change by actions through a rule-based ontology and built a knowledge base from natural language. We focus on “active perception” [16] to realize the recognition of both extrinsic and intrinsic characteristics “by the robot itself”. Active perception allows recognition of the target ingredient characteristics by capturing time-series changes in sensory information while directly acting on and interacting with a target [17], [18]. We allow the robot to interact with the target ingredient to recognize its characteristics while performing cooking motions.

To recognize both extrinsic and intrinsic characteristics with active perception, multimodality, i.e., vision, tactile, and force sense, is required [19], [20]. However, important modalities switch rapidly, as shown in Fig. 2: when the target is visually occluded by the robot arm itself, the robot must focus on tactile and torque; in contrast, when the robot does not touch the target, the robot should focus on images. Some previous research has focused on the perception of characteristics using multimodality [21], [22], however they only allow robots to handle stable targets that do not considerably change their state during motions. Some studies have focused on deformable targets such as liquids, however they had to control the robots to conduct pre-defined exploring motions in the beginning to perceive the object characteristics before starting the target motions [23]–[25]. We hypothesize that the difficulty occurs because the robots cannot perceive characteristics and generate motion quickly and efficiently enough for handling real-time changes. Therefore, to enable the robots to perceive and handle changing ingredients efficiently, we propose a learning model that can distinguish the reliability and importance of the modalities. We introduce an attention mechanism that can weigh the modality in a predictive deep learning model considering the reliability and importance at that time. While much previous research has used attention mechanisms to detect gaze points

in images or for visual explanation [26]–[28], we use the mechanism for multimodal data to map the importance of the information.

To make a robot complete the “desired” daily dexterous manipulation tasks, learning humans’ “skills” for the goal is necessary. To learn humans’ skill, learning from demonstration (LfD) [29], [30], which allows the robot to learn the action from expert examples without explicitly indicated commands, is critical, like other cooking robotics and dexterous manipulation research as [31]–[34]. We collected expert demonstration data with teleoperation by humans and allowed the robot to acquire human cooking skills through LfD. In our cooking scenario, we set the following goals for cooking scrambled eggs as follows: (1) separate egg blocks no larger than 15 cm, (2) do not burn, and (3) heat well so that no raw egg remains. Cooking a scrambled egg that meets all goals (1)-(3) is very challenging. When the robot replayed the training data trajectory or moved randomly in the pot, it left some raw parts, while the other parts had burned, and could not separate the egg well. In addition, some blocks’ size was large. Surprisingly, even though the replayed motion was the same as the teleoperated one used for training data, the robot could not cook the scrambled egg to meet all conditions. To cook a scrambled egg with the goal skills, the robot must update its perception and generate motion in real time.

Fig. 3 shows the architecture of the LfD model. The model is composed of a convolutional autoencoder (CAE) [35] for image feature extraction and an MTRNN [36] for motion generation. Since the dimension of the image data is much larger than that of other sensors, we use CAE to compress it. Subsequently, all data is concatenated and input to the MTRNN. The robot is controlled by the predicted motor angle data, which is outputted from the MTRNN. To distinguish between the importance of the modalities at every moment, an attention mechanism is introduced in the MTRNN. The MTRNN is composed of two context nodes with different time constants in addition to input-output (IO) node: the slow context (Cs) node with the largest time constant learns sequential data, and the fast context (Cf) node with a small time constant learns primitive data. We insert the attention mechanism between IO and Cf nodes. The attention mechanism distinguishes between the importance of the multimodal input data, which is the key based on the contextual historical information in the Cf as the query, and weighs the input data as the value, as shown in 4. In other words, the attention mechanism works as a filter to pass data from the IO node to the Cf node.

To demonstrate the effectiveness of the proposed model, we used the humanoid robot, Dry-AIREC, developed by Tokyo Robotics Inc. [37], [38]. We controlled the robot’s right arm which has 7 DOF with impedance control. We used an induction cooker used in real home kitchen environments and asked the robot to cook, as shown in Fig. 1.

The robot learned cooking using 32 datasets with teleoperation with the egg mixture, adding four different ingredients, as shown in Fig. 5, and using two different heating

TABLE I: Success rate of cooking scrambled egg with training ingredients

heating power	plain	seaweed	corn	sausage	total
180°C	5/5	4/5 (push out)	4/5 (block)	4/5 (block)	17/20
190°C	5/5	4/5 (push out)	5/5	5/5	19/20
total	10/10	8/10	9/10	9/10	36/40

(): reason of failure

temperatures. As a result, the robot could cook scrambled eggs automatically in 90.0% (36/40) of the cases, as shown in Table I. The model performed generalization of ingredient characteristics, and the robot succeeded in cooking the eggs using six different unknown ingredients with a high success rate, 78.3 % (47/60), as shown in Table II. With our proposed model, the robot could change the method of stirring and direction depending on the status of the egg, as in the beginning it stirs in the whole pot, then subsequently, after the egg started being heated, the robot starts flipping and splitting motion targeting specific areas, although we did not explicitly indicated them.

We performed a survey on the appearance and taste of the scrambled eggs. We took pictures of the dishes cooked by humans and the robot with our model, and asked the respondents to distinguish them. As a result, the success rate for the distinction was 56.6 %, indicating that the robot could cook dishes similar to humans in appearance. We also asked the respondents to grade the dishes cooked by humans, by robots with our proposed model, and by robots without the model in order. As shown in Table III, our model scored well in terms of appearance of the eggs, and the ratings were almost the same as those for the human-made eggs. Thus, using our model, the robot could acquire good cooking skills similar to those of humans.

From our analysis, we confirmed the attention mechanism distinguishes important modality at that time based on the egg status and necessary action, which is necessary for the real time cooking. In addition, we found that the latent space in the LfD model explains the egg status from raw to hard, and provides the complete time of cooking. We concluded that our LfD model with attention mechanism is critical to realize real time motion generation with active perception, which is necessary for manipulating deformable objects whose states change continuously.

II. RESULTS

A. Success rate of cooking

Table I shows the results of the accuracy of the trained model for the egg mixture. We performed 40 trials, and in total, 36 (90.0 %) trials met all rules: (1) no egg block larger than 15 cm, (2) no burned parts, and (3) no raw parts. The table also shows the reasons for failure. With the plain egg mixture, which is the simplest one, the robot succeeded in all trials. While with seaweed, the robot pushed out the pan in two trials, which is because the color of seaweed is dark blue, the CAE was difficult to distinguish between the seaweed and

the black pot. In the trial with a heating power of 180 °C, one trial each with seaweed, corn, and sausage, some large blocks remained in the pan and failed. Cooking at a heating power of 180 °C is more difficult than cooking at 190 °C. At 180 °C, it takes more time for the egg to harden, and the egg can easily stick to the other egg blocks again even after the robot has split the egg block.

Table II shows the results of robustness evaluation using untrained ingredients. We performed 60 trials, and in total, succeeded 47 (78.3 %) times. The way to stir and the time to cook differs depending on the ingredients; however, the robot could recognize the characteristics and adjust them flexibly. The egg with cheese trial was especially difficult because cheese is sticky and stretchy, and its characteristics are considerably different from those of ingredients used for training; however, the model succeeded in 6/10 trials. We concluded that the model has acquired good generalization ability.

B. Action change depends on egg status

Fig. 7 shows that the robot cooked plain eggs at a temperature of 190 °C. First, as shown in the picture, in the beginning, the robot stirred in a circle along the rim of the pot, expecting the robot to recognize the characteristics of the egg. Second, in the 49th and 66th time step, while the egg was still raw, the robot stirred largely all over the pan. Subsequently, after the egg started being heated, the robot started flipping motion at the 244th time step. Next, when almost all parts had hardened as 360th time step, the robot cut the large egg block and split them. These motions are not explicitly indicated but the LfD model learn it implicitly and acquire the cooking skill from human demonstrations.

We also show the reconstructed whole/trimmed images by the CAE. The whole images show and represent the arm postures, and the trimmed images show the egg status. Especially, the trimmed images show which part of the egg is separated or connected. Thus we can assume that the CAE could recognise the status of the egg and the robot arm.

C. Acquisition of skills

We administered two questionnaires to evaluate the appearance and taste of the cooked dish to confirm if the robot could acquire cooking skills similar to humans.

In Questionnaire-1, we showed pairs of images of the dish humans cooked and the dish that the robot cooked with our proposed model to the respondents and asked them to identify the robot-made dish. We asked seven people to cook and controlled the robot to cook seven times. We randomly selected one of each seven pictures 14 times, and made 14 pairs for the survey. Then, we administered the survey to 25 respondents. As a result, the respondents successfully distinguished human-made dishes in 56.6% (198/350 pairs) cases. That is not very far from 50%; thus, we can say the robot could cook almost similar to humans.

In Questionnaire-2, we showed a set of real dishes or images of dishes (human-made / robot-made with our model / robot-made but cooked with just replaying the training

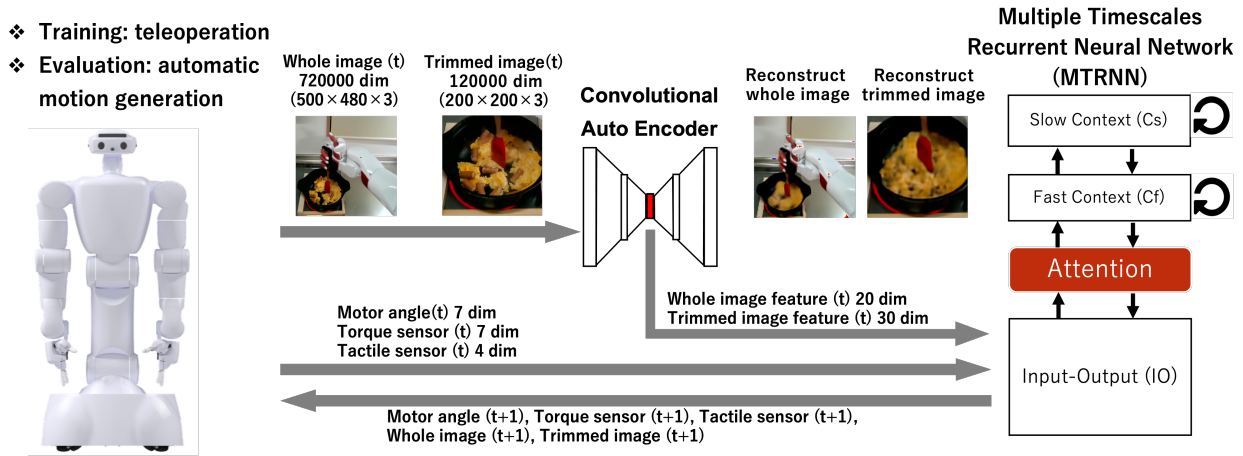


Fig. 3: The proposed LfD model is composed of a CAE, which extracts image features, and a MTRNN with the attention mechanism, which conducts predictive learning considering the importance of each modality.

TABLE II: Success rate of cooking scrambled egg with UNTRAINED ingredients

heating power	vision		touch		vision & touch		total
	say source	red food coloring	bamboo shoots	cheese	minced meat	spinach	
180°C	5/5	4/5 (block)	3/5 (blocks)	4/5 (block)	3/5 (blocks)	4/5 (block)	23/30
190°C	4/5 (block)	5/5	4/5 (burn)	2/5 (push out, block, burn)	5/5	4/5 (block)	24/30
total	9/10	9/10	7/10	6/10	8/10	8/10	47/60
	18/20		13/20		16/20		

(): reason of failure

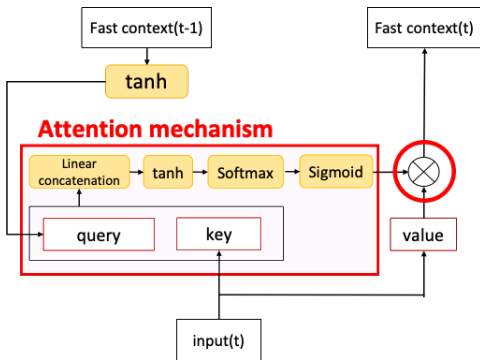


Fig. 4: Attention mechanism which is introduced inside the MTRNN. The attention mechanism can pass important modality information to context.

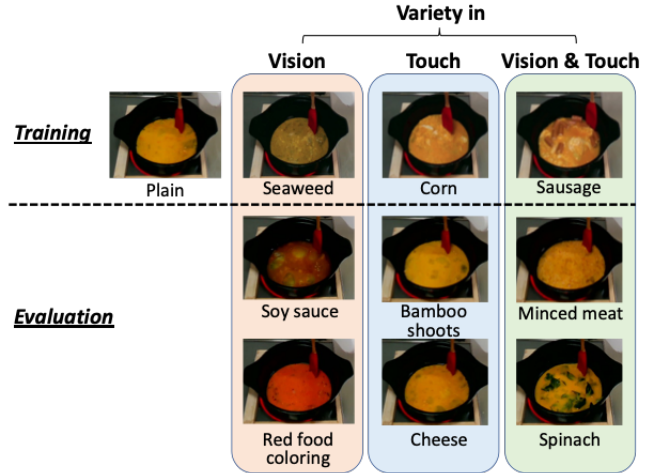


Fig. 5: Variation in the egg mixture, which is used for training and evaluation.

motion) to the respondents, as shown in Table III. We asked them to order and grade the dishes with the highest three points given to the best one. Twenty-five respondents were included in the survey with images, and nine in that with the real dishes; we asked them to evaluate not only the appearance but also the taste. As a result, for the appearance of both images and real dishes, the images of robot-made dishes with our model scored as high as human-made dishes and much higher than the replay-training dishes. Thus, we can say the robot acquired the skill to cook appealing scrambled eggs. However, as for taste, there was no considerable difference among the three, because the taste depends on

the respondents' preferences, with some people liking harder eggs than others, which altered the score of replay-training. Cooking according to the person's taste preference is the next challenge.

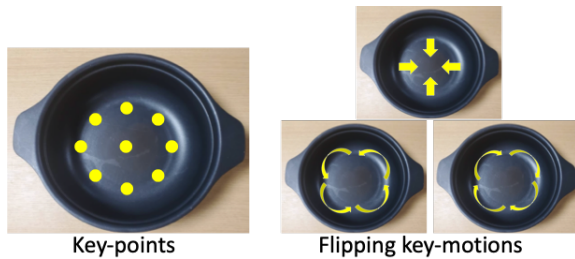





Fig. 6: Key points and key flip motions to command to the robot during teleoperation for collecting training data.

TABLE III: Result of Questioner-2: grade the dish with appearance and taste

	humans made	with our model	replay training
appearance with images	 62 points	 63	 25
appearance of real dish	29	28	15
taste of real dish	27	21	24
total	118	112	64

25 participants for appearance with pictures, 12 participants for the rest.
Grade 1st: 3 points, 2nd: 2 points, 3rd: 1 point

III. DISCUSSION

A. The effect of the attention mechanism with trajectory analysis

To confirm our model’s effectiveness, we tried the same CAE and the MTRNN architecture after removing the attention mechanism. Without the attention mechanism, we controlled the robot to cook plain eggs by heating at 190 °C, over five trials, which is the condition all trials succeeded with our model. As a result, in 4 trials, the robot pushed and hit the pot wall with too much force and stopped movement because it exceeded the safety torque limit. In one trial, the robot only stirred the right area in the pot, where the arm did not occlude the pot and the egg was visible. Thus, we assume that without the attention mechanism, the robot cannot focus on torque and tactile sensor information, which makes it difficult to return to the other direction just after the turner hits the pot wall. Moreover, the model without attention mechanism focuses on vision too much, thus the robot only stirred the observable position.

With Kinovea [39], a motion analysis software, we analyzed the stirring trajectory and compared the trained model, our LfD model, and without attention model, as shown in Fig. 8. We tracked the tips of the turner with the software and showed the trajectory in the videos of the robot view. They are all in the case the robot stirred plain egg with heating 190 °C. With our LfD model shown in the middle figure of Fig. 8, the trajectory covers all the area in the pot as training data. In addition, the trajectory shows that at first,

the robot stirs roundly with large motion to approach the whole area. Then gradually changed to sharp motion to flip or split targeting the specific areas. In the right figure, we show the model without attention, in which the robot only stirred the right area of the pot, because of which, a large block was not stirred on the left side and burned. Therefore, we can say that the attention mechanism is critical to adjust the movement depending on the objects’ complex changing characteristics.

B. Detecting important modality with Attention map analysis

We analyzed the attention mechanism to confirm the focused modalities each time. In Fig. 9, Fig. 10, and Fig. 11, we show attention maps, which are heat maps representing the attention weight, which is output from the attention mechanism, the red square in Fig. 4. The values in these figures are normalized, and the lighter color indicates a highly focused modality, which the LfD model recognise as important and reliable. They are all in the case the robot stirred plain egg with heating 180 °C.

Fig. 9 is the attention map of the whole dimensional data. Lines around the 148, 186, 242, 300, 347, and 425 steps can be seen. We can see the transition of focused sensorimotor data. In these time steps, occlusion occurred, as shown in the pictures in the Fig. 9. We can assume that the DNN model recognizes the occlusion and changes the focus depending on the situation.

Fig. 10 shows the attention map averaged with each modality. As can be seen, especially the heat color of torque sensor data becomes lighter and lighter, which means it attains focus in the latter half of the sequence. We consider that that is because in the latter half, the egg became harder; thus, the LfD model must focus on recognizing which part is soft or hard. In contrast, the attention towards the whole image data diminishes in the last part. In the beginning, the robot has to move largely to stir the whole pot, but later, the movement becomes small and involves flipping or splitting a specific area, which mainly needs wrist transition. Thus, the whole image becomes less and less meaningful.

Fig. 11 shows the attention map with only joint angle data. We can see that joints 2, 4, and 5 decrease attention, which are mainly used for stirring in the whole pot. In contrast, joints 3, 6, and 7 increase attention, which are used for splitting the egg. We can say that the attention mechanism can focus on important joints based on the egg status and necessary action type.

C. Detecting egg status with PCA

We conducted principal component analysis (PCA) on the sequential Cs internal value in MTRNN while conducting the evaluation experiment, as shown in Fig. 12. There are seven nodes in the Cs node, but with PCA, we can analyze the information represented in Cs with 3 dimensions. Fig. 12 shows two samples for each heat power and ingredient; the left figure shows the sequence until 520 steps, which is the timing only when heating with 190 °C finish cooking, and the right figure shows until 640 steps, which is the timing of

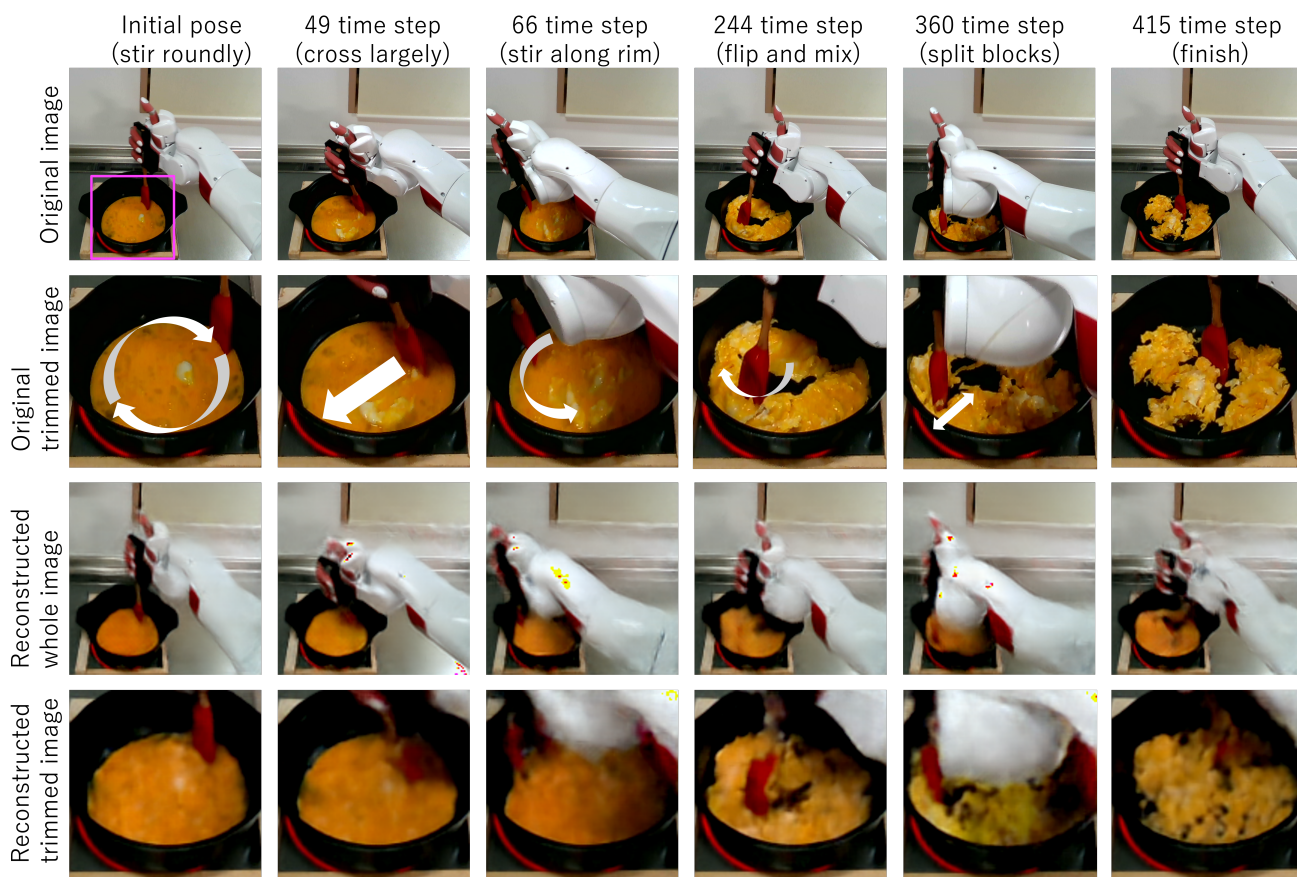


Fig. 7: The robot generated motions with our model and succeeded in cooking scrambled eggs using plain eggs, heating with 190 °C. The original images and reconstructed images are shown. The purple squared area is used as the trimmed image. The robot performed stirring, flipping, and splitting according to the situation.

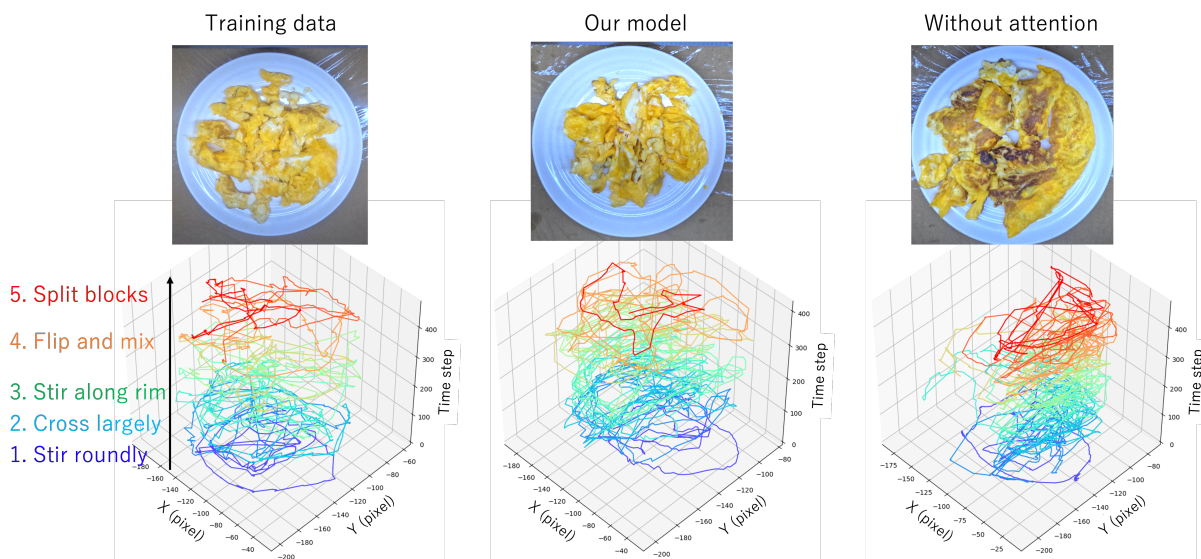


Fig. 8: The cooked dishes and traced stirring trajectories to compare the training data, our model, and without-attention model, with plain eggs, 190 °C. Our model could cover the whole pot as training data, whereas the model without attention mechanism stirring mainly covered the right side of the pot, which makes the pot always visible. In addition, the trajectories of training data and our model show that the motions approach the whole area at first but gradually changed to sharp targeting of specific areas.

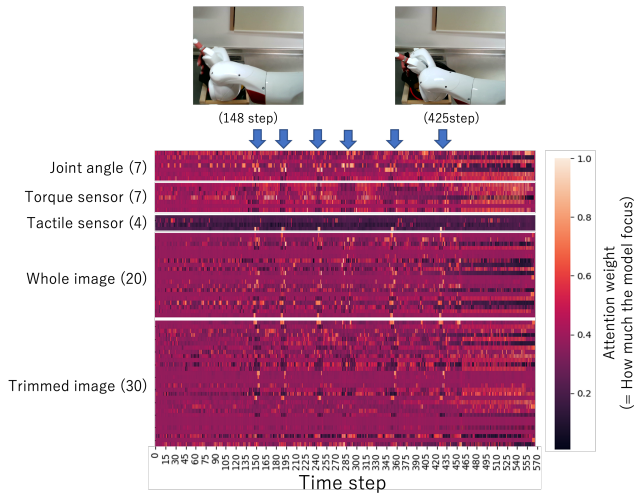


Fig. 9: Attention map of the whole dimensional data while the robot is cooking with plain eggs, heating with 180 °C. There is a switch of focused dimension when occlusion occurs, which is represented with vertical wave lines in the figure.

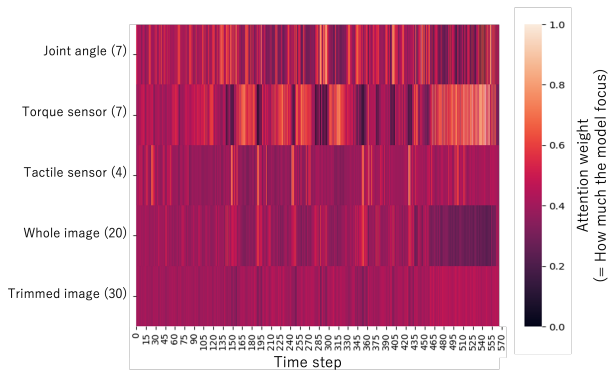


Fig. 10: Attention map averaged with each modality. Torque sensor data gathers focus in the latter half; in contrast, whole images lose attention at the end.

most of trials with heating with 190 °C also finish cooking. In both figures, all sequential plots transition from minus to plus in the PC1 axis, which can explain the egg status, from raw to hard. In other words, the PC1 axis represents egg status. On the left, with 190 °C, all the flow has reached the plus side; however, with 180 °C trials, all of them have not moved from the minus side, since at the 520th step, only eggs heated with 190 °C can harden. In conclusion, we can assume that the Cs node represents egg status and provides the complete time of stirring, which enable robot to complete the cooking task.

D. Future works

There are some areas for future work. First, as for cooking, food quality, as related to aspects such as taste, texture, and flavour is critical [8], [40]. Moreover, food preferences also differ from person to person. We conducted questionnaires but will investigate the way to evaluate personal preference

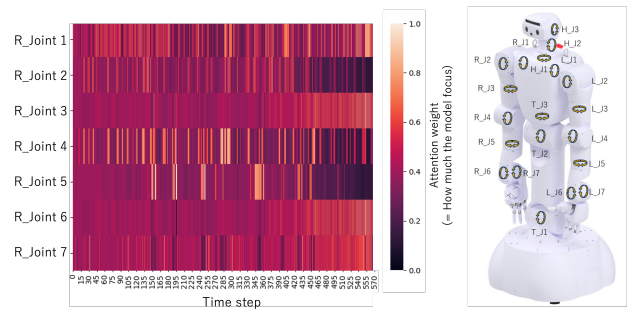


Fig. 11: Attention map only shows joint data. Joints 2, 4, and 5 decrease attention, which are mainly used for stirring largely in the whole pot. Joints 3, 6, and 7 increase attention because they are used for splitting egg motions.

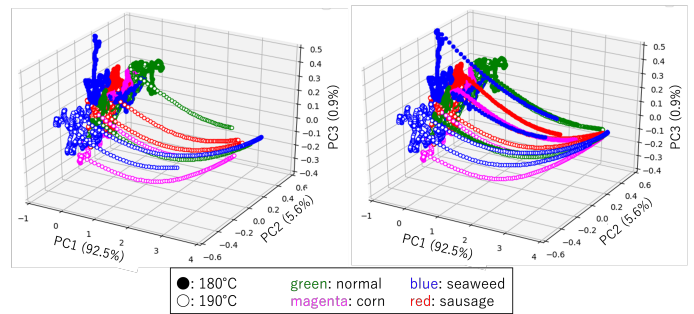


Fig. 12: PCA of sequential Cs internal value during cooking. We show 2 samples for each heat power and ingredient. The left figure shows the sequence until 520 steps and the right figure shows until 640 steps. The plots flow from minus to plus along the PC1 axis, which explains the egg status, from raw to hard. We can assume that the Cs node provides the complete time of stirring based on the status.

and propose a system that can serve dishes depending on the person’s preference.

Second, long-horizontal cooking manipulation composed of several procedures is the next target. Although cooking scrambled eggs involves numerous procedures such as taking eggs from a fridge, cracking the eggs, breaking the yolk and making the egg mixture, pouring the mixture into the pan, stirring the pan while heating it, and serving on a plate, we realized only pouring (with the fixed motion) and stirring (with motion generation). There is some research on cooking according to recipes [41], [42] from which we can obtain insights. Some previous studies focused on long-horizon manipulation using a large language model (LLM) to order the task [43] and proposed a motion planning method to consider the way and the order to conduct actions [44], [45]. We are planning to utilize the latent space of LfD model as attention mechanism and Cs nodes to predict states and next actions as in [11], [46], [47], which will agree with our proposed LfD model.

Moreover, understanding each procedure semantically is important [48], [49]. In the future, we will establish a cooking robot system tailored to personal preferences. To achieve

TABLE IV: Structure of the CAE

	Input	Output	Activation	Processing
1	(128, 128, 3)	(64, 64, 8)	ReLU	convolution
2	(64, 64, 8)	(32, 32, 16)	ReLU	convolution
3	(32, 32, 16)	(16, 16, 32)	ReLU	convolution
4	25,088	1,000	ReLU	fully connected
5	200	MID	Sigmoid	fully connected
6	MID	200	ReLU	fully connected
7	1,000	25,088	ReLU	fully connected
8	(16, 16, 32)	(32, 32, 16)	ReLU	deconvolution
9	(32, 32, 16)	(64, 64, 8)	ReLU	deconvolution
10	(64, 64, 8)	(128, 128, 3)	ReLU	deconvolution

MID = 20: whole images, 30: trimmed images

this vision, the robot must predict the cooking procedures and adjust each task considering how to satisfy personal preference not just follow a recipe or human orders.

Finally, simulation-use is necessary [50], [51]. Conducting all experiments with a real robot in a real environment was challenging. We would like to collect data in simulation with enough quality and establish a system for simulation-to-real.

IV. METHODS

A. Module overview

Fig. 3 shows the whole architecture of the proposed deep learning model. It is composed of two modules, the CAE, which extracts image features, and the MTRNN, which integrates all sensorimotor information and generates motions. We integrated an attention mechanism into the MTRNN to pass the sensorimotor data, giving weight based on its importance to context nodes.

1) *Image feature extraction using CAE*: We used the CAE to compress images to low-dimensional features such that the MTRNN could learn all sensorimotor data in a well-balanced manner. It was trained to make the output reconstructed data ($y^{\text{Img}}(t)$) identical to the input data ($x^{\text{Img}}(t)$) by minimizing the mean squared error (MSE) shown below with the optimizer for the Adaptive moment estimation (Adam) algorithm [52].

$$E = \frac{1}{N} \sum_t (y^{\text{Img}}(t) - x^{\text{Img}}(t))^2. \quad (1)$$

Table IV lists the structural parameters used for constructing the CAE. We used the value of the intermediate layer as the image features ($y^{\text{Img}}(t) = x^{\text{ImgFeature}}(t)$). We set the number of the intermediate layer neurons to 20 for the whole images and to 30 for the trimmed images. We tested changing the numbers of the intermediate layer nodes by 15, 20, ..., 35 and set the number so that it was the smallest number in which output ($y^{\text{Img}}(t)$) could sufficiently reconstruct the original image ($x^{\text{Img}}(t)$). The convolution was conducted using a 6×6 kernel, 2 strides, and 1 zero padding. This module was trained for 1,500 epochs.

2) *Motion generation using MTRNN with attention mechanism*: We used the MTRNN as the main module to integrate all sensorimotor data, recognize the current egg states, and generate motions accordingly. The MTRNN is a recurrent neural network that predicts the next step from the current

TABLE V: Structure of the MTRNN

Nodes	Time constant	Number of nodes
C_s	32	7
C_f	5	30
IO	2	68

and previous inputs. It has multiple nodes with different time constants; it not only has IO nodes but also C_s (C_s) and C_f (C_f) nodes. The C_f nodes can learn short-term primitive data because of their small time constant, while the C_s nodes with a large time constant can learn the sequential information and behave as the latent space. Table V shows the time constants and number of nodes used in the study, which are the best combinations to minimize the error which will be described in Eq. (7).

In this research, we originally implemented an attention mechanism in the MTRNN. We make the value of IO nodes ($x_{\text{IO}}(t)$) as the “key”, and the internal value of C_f nodes in the previous step ($u_{C_f}(t-1)$) as the “query” and the “value,” respectively. Using the key and the query, the attention mechanism ($A(t)$) is calculated as follows and represents the map of the focusing factor of the key.

$$A(t) = \text{sigmoid} \left(\text{softmax} \left(\tanh(x_{\text{IO}}(t), u_{C_f}(t-1)) \right) \right) \quad (2)$$

The attention mechanism is multiplied with the value, and the weighted value of IO nodes ($x_{\text{IO}}(t)$) is utilized for the internal value of C_f nodes in the current step ($u_{C_f}(t)$).

Forward calculations are described as follows. First, input data $T(t)$, which is either the training data during model training or the real-time data during evaluation experiments. The input data is the image features, which is output from CAE, torque sensor data ($x^{\text{Tor}}(t)$), tactile sensor data ($x^{\text{Tac}}(t)$), and motor angle data ($x^{\text{Mot}}(t)$). Input to IO nodes of MTRNN ($x_{\text{IO}}(t)$) is combination of $T(t)$ and prediction from the previous step, which is described later in Eq. (6).

$$T(t) = [x^{\text{ImgFeature}}(t), x^{\text{Tor}}(t), x^{\text{Tac}}(t), x^{\text{Mot}}(t)] \quad (3)$$

The internal value u_i of the neuron i at step t is calculated as follows. The internal value of C_f nodes in the current step ($u_{C_f}(t)$) is calculated with attention mechanism.

$$u_i(t) = \begin{cases} (1 - \frac{1}{\tau_i})u_i(t-1) + \frac{1}{\tau_i} [\sum_j w_{ij}x_j(t)] & i \in \text{IO}, C_s \\ (1 - \frac{1}{\tau_i})u_i(t-1) + \frac{1}{\tau_i} [w_{i,\text{IO}}\{A(t)x_{\text{IO}}(t)\} + w_{i,C_s}x_{C_s}(t)] & i \in C_f, \end{cases} \quad (4)$$

where j is the other nodes connected to each node i , τ_i is the time constant of node i , w_{ij} is the weight value from node j to node i , and $x_j(t)$ is the input value of node i from node j . Subsequently, the output value is calculated as

$$y_i(t) = \tanh(u_i(t)). \quad (5)$$

Using the output, the module can generate robot motions by controlling the movements of the robot according to the

output motor angle ($y_i^{\text{Mot}}(t)$). Subsequently, the value of $y_i(t)$ is used as the next input value, which is expressed as

$$x_i(t+1) = \begin{cases} \alpha \times y_i(t) + (1 - \alpha) \times T(t+1) & i \in \text{IO} \\ y_i(t) & i \in \text{Cf, Cs.} \end{cases} \quad (6)$$

The next input value $x_{\text{IO}}(t)$ is adjusted by multiplying the output of the preceding step $y_{\text{IO}}(t-1)$ and the data $T(t)$ by the feedback rate α ($0 \leq \alpha \leq 1$). If the feedback rate is high, the model can stably predict the next step using own prediction history, whereas if the value is small, the model can flexibly adapt to real-time situations more sensitive to the real data. We set the feedback rate 0.9 during training, on the other hand during the evaluation, we set 0.8 as the motor angle ($x^{\text{Mot}}(t+1)$) and 0.6 for others ($x^{\text{ImgFeature}}(t+1)$, $x^{\text{Tor}}(t+1)$, $x^{\text{Tac}}(t+1)$).

To realize backward calculations during training, the back propagation through time (BPTT) algorithm was used to minimize the training error as,

$$E = \sum_t ((y_{\text{IO}}(t-1) - T(t))^2) \quad (7)$$

The weight is updated as

$$w_{ij}^{n+1} = w_{ij}^n - \eta \frac{\partial E}{\partial w_{ij}^n}, \quad (8)$$

where $\eta (= 0.001)$ is the learning rate and $n (= 20,000)$ is the number of epochs.

B. Training method

The sensorimotor training data were collected while the robot was teleoperated to cook scrambled eggs. We set nine keyposes in the pot and prepared specific flipping motions as shown in Fig. 6. An experimenter commands the keyposes or flipping motions to the robot to control it while the person checks the egg status through the monitor showing the view of the robot.

The experimenter teaches the target cooking motion and cooking skills to the robot through teleoperation. The operator controls the robot and cooks the scrambled egg with the following in mind. At first, when the egg is totally raw, the operator makes the robot stir largely to cover the whole pot. Then, when some part of the egg starts becoming hard, the operator makes the robot starts approaching the hard part and flips the egg to prevent it from burning and to ensure all parts are heated evenly. Finally, when the entire egg has hardened, the large mass is sliced and separated.

C. Hardware and control

The humanoid robot, Dry-AIREC, has 7 DOF dual arms, and all of the joints have a torque sensor. We used a RGB camera, RealSense TM SR300, attached to its head. On its hand, a touch sensor, FSR406, was attached to each of the four fingers and the palm. We used three fingers except for the thumb, which does not touch the turner. The robot was controlled using impedance control.

D. Task setting

The task was to cook a scrambled egg aiming to make it similar to dishes that humans make, which met all rules: (1) no egg block larger than 15 cm, (2) no burned parts, and (3) no raw parts. We conducted the cooking experiment by changing the heating power to 180 and 190 °C and the ingredients that were mixed with the egg mixture, which influenced the speed and area to be heated.

The robot was set in a kitchen of a usual living space. It grabbed a pitcher which contained an egg mixture with its left hand and a turner for stirring the egg with its right hand. At first, the pot is heated with an induction cooker with a certain heating power (180 and 190 °C) for 60 sec. Then, the robot pours the egg mixture into the pot with its left hand, which is controlled by a pre-designed motion. Subsequently, the robot starts stirring with its right hand controlled by the proposed LfD model. If the LfD model detects the completion of cooking the right arm remains stationary and signals its completion.

E. Dataset

Fig. 5 shows the variation in the egg mixture used for the experiments. We trained with 4 types of egg mixtures: plain and with 1 g of seaweed, 100 g of corn, and 10 sticks of sausage. We selected them to observe differences in only vision, only touch, and both vision and touch. As for evaluation, we prepared unknown ingredients: 10 g of soy source and 0.3 g of red food coloring which has differences in vision; 50 g of bamboo shoots and 15 g of natural cheese which has differences in touch; and 100 g of minced meat and 15 g of spinach which has differences in both vision and touch.

To train the LfD model, we collected 32 datasets: (4 types of egg mixtures) \times (2 heating power) \times (4 trials). The data were sampled at 2.5 Hz and recorded every 0.4 sec. The time length to cook was 248 sec on average (620 time steps) for 180 °C and 182 sec (455 time steps) for 190 °C. The dimensions of the sensorimotor data we input into the LfD model are as follows. As for the images, we used whole images (500 W \times 480 H \times 3 C) and trimmed images (200 W \times 200 H \times 3 C), which focus on the inside of the pan. They were first converted to size (128 W \times 128 H \times 3 C), normalized to [0, 1], and input to the CAE. In addition, we used tactile sensor data (4 points; attached on first, second, and third fingers and palm), torque sensor data (7 points attached in each joint), and motor angle data (7 joints), which were normalized to [-0.85, 0.85], [-0.9, 0.9], and [-0.9, 0.9], respectively. The range of normalization was adjusted based on the amount of vibration and noise.

V. APPENDIX

A. Tried cooking different dishes

We focused on cooking totally different dishes, as shown in Fig. 13. The robot succeeded in stirring stir-fried rice, mixed vegetables, and white stew. Even though the states of the ingredients change differently from those of the egg, the robot showed movements approaching to and separating

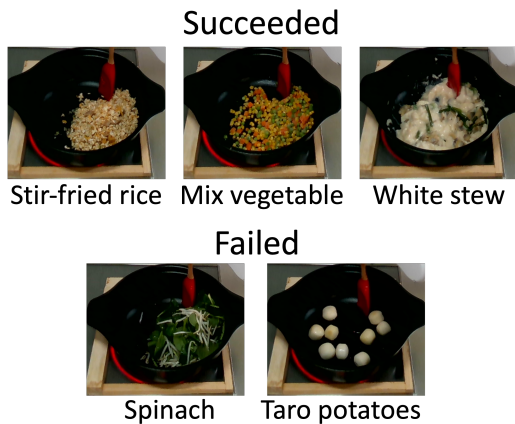


Fig. 13: Tested dishes that were different from scrambled eggs.

the gathering parts. The robot could even decide the end timing of the motion, which is when the stir-fried rice and vegetables become softer, and the white stew became smoother. Therefore, we assume that the LfD model has a good generalization potential ability to recognize the transition of the states and decides motion and end timing.

However, the robot failed to stir some samples: the spinach and the taro potatoes. This is because the spinach is dark and difficult to distinguish from the pot. Regarding the taro potatoes, we assume that they are difficult to stir because they rotate and bump easily, which leads to a drastic difference in tactile sensing, and they are visually sparse; thus, the robot may assume the pot to be empty. If there is a considerable difference from the trained data in sensing, it is difficult to generalize. Generalization to ingredients with much different characteristics is one of our future works.

B. Tried with different heat power

The induction cooker can adjust heating with every 10 °C, and in the training and evaluation experiments, we used heat with 180 °C and 190 °C. In the additional experiment, we tried cooking at 170 °C. (Heating at 200 °C burns the egg very easily, and cooking at this temperature is difficult even for humans, so we did not attempt the higher heating power.) At 170 °C, the state of the egg mixture changes slowly, and it takes much longer to harden. We tested three trials, and in two trials, the robot detected the end timing and stopped stirring before the pan was fully heated, and some raw parts remained. However in one trial, the robot succeed in cooking. We confirmed the possibility of generalizing to other heating powers, which led to totally different behaviors of the ingredients.

REFERENCES

[1] K. Yamazaki, R. Ueda, S. Nozawa, M. Kojima, K. Okada, K. Matsumoto, M. Ishikawa, I. Shimoyama, and M. Inaba, “Home-assistant robot for an aging society,” *Proceedings of the IEEE*, vol. 100, no. 8, pp. 2429–2441, 2012.

[2] E. Guizzo and E. Ackerman, “The rise of the robot worker,” *IEEE Spectrum*, vol. 49, no. 10, pp. 34–41, 2012.

[3] F. Cavallo, R. Limosani, A. Manzi, M. Bonaccorsi, R. Esposito, M. Di Rocco, F. Pecora, G. Teti, A. Saffiotti, and P. Dario, “Development of a socially believable multi-robot solution from town to home,” *Cognitive Computation*, vol. 6, pp. 954–967, 2014.

[4] S. J. Lederman and R. L. Klatzky, “Hand movements: A window into haptic object recognition,” *Cognitive Psychology*, vol. 19, no. 3, pp. 342–368, 1987.

[5] R. S. Dahiya, G. Metta, M. Valle, and G. Sandini, “Tactile sensing—from humans to humanoids,” *IEEE Transactions on Robotics*, vol. 26, no. 1, pp. 1–20, 2010.

[6] T. Bhattacharjee, G. Lee, H. Song, and S. S. Srinivasa, “Towards robotic feeding: Role of haptics in fork-based food manipulation,” *IEEE Robotics and Automation Letters*, vol. 4, no. 2, pp. 1485–1492, 2019.

[7] W. X. Yan, Z. Fu, Y. H. Liu, Y. Z. Zhao, X. Y. Zhou, J. H. Tang, and X. Y. Liu, “A novel automatic cooking robot for chinese dishes,” *Robotica*, vol. 25, no. 4, p. 445–450, 2007.

[8] K. Junge, J. Hughes, T. G. Thuruthel, and F. Iida, “Improving robotic cooking using batch bayesian optimization,” *IEEE Robotics and Automation Letters*, vol. 5, no. 2, pp. 760–765, 2020.

[9] S. Yang, M. Chen, D. Pomerleau, and R. Sukthankar, “Food recognition using statistics of pairwise local features,” in *2010 IEEE Computer Society Conference on Computer Vision and Pattern Recognition*, 2010, pp. 2249–2256.

[10] A. Petit, V. Lippiello, G. A. Fontanelli, and B. Siciliano, “Tracking elastic deformable objects with an rgb-d sensor for a pizza chef robot,” *Robotics and Autonomous Systems*, vol. 88, pp. 187–201, 2017.

[11] X. Lin, C. Qi, Y. Zhang, Z. Huang, K. Fragkiadaki, Y. Li, C. Gan, and D. Held, “Planning with spatial-temporal abstraction from point clouds for deformable object manipulation,” in *6th Annual Conference on Robot Learning*, 2022.

[12] M. S. Salekin, A. B. Jelodar, and R. Kushol, “Cooking state recognition from images using inception architecture,” *2019 International Conference on Robotics, Electrical and Signal Processing Techniques (ICREST)*, pp. 163–168, 2019.

[13] J. Gao, B. Sarkar, F. Xia, T. Xiao, J. Wu, B. Ichter, A. Majumdar, and D. Sadigh, “Physically grounded vision-language models for robotic manipulation,” in *arXiv preprint arXiv:2309.02561*, 2023.

[14] M. Tenorth and M. Beetz, “A unified representation for reasoning about robot actions, processes, and their effects on objects,” in *2012 IEEE/RSJ International Conference on Intelligent Robots and Systems*, 2012, pp. 1351–1358.

[15] D. Nyga and M. Beetz, “Everything robots always wanted to know about housework (but were afraid to ask),” in *2012 IEEE/RSJ International Conference on Intelligent Robots and Systems*, 2012, pp. 243–250.

[16] R. Bajcsy, “Active perception,” *Proceedings of the IEEE*, vol. 76, no. 8, pp. 966–1005, 1988.

[17] Q. Le, V. A. Saxena, and Y. A. Ng, “Active perception: Interactive manipulation for improving object detection,” *Stanford University Journal*, 2008.

[18] P. Benjamin, D., D. Lonsdale, and D. Lyons, “Designing a robot cognitive architecture with concurrency and active perception,” *Proceedings of the AAAI Fall Symposium on the Intersection of Cognitive Science and Robotics*, 2004.

[19] M. O. Ernst and M. S. Banks, “Humans integrate visual and haptic information in a statistically optimal fashion,” *Nature*, vol. 415, no. 6870, pp. 429–433, 2008.

[20] H. Liu, Y. Yu, F. Sun, and J. Gu, “Visual–tactile fusion for object recognition,” *IEEE Transactions on Automation Science and Engineering*, vol. 14, no. 2, pp. 996–1008, 2017.

[21] M. C. Gemici and A. Saxena, “Learning haptic representation for manipulating deformable food objects,” in *IEEE/RSJ International Conference on Intelligent Robots and Systems (IROS)*, 2014.

[22] P. Sundaresan, S. Belkhale, and D. Sadigh, “Learning visuo-haptic skewering strategies for robot-assisted feeding,” in *6th Annual Conference on Robot Learning*, 2022.

[23] N. Saito, T. Ogata, S. Funabashi, H. Mori, and S. Sugano, “How to select and use tools? : Active perception of target objects using multimodal deep learning,” *IEEE Robotics and Automation Letters*, vol. 6, no. 2, pp. 2517–2524, 2021.

[24] N. Saito, N. B. Dai, T. Ogata, H. Mori, and S. Sugano, “Real-time liquid pouring motion generation: End-to-end sensorimotor coordination for unknown liquid dynamics trained with deep neural networks,”

- in *IEEE International Conference on Robotics and Biomimetics (RO-BIO)*, 2019.
- [25] T. Lopez-Guevara, R. Pucci, N. K. Taylor, M. U. Gutmann, S. Ramamoorthy, and K. Subr, “Stir to pour: Efficient calibration of liquid properties for pouring actions,” *IEEE/RSJ International Conference on Intelligent Robots and Systems (IROS)*, 2020.
- [26] H. Fukui, T. Hirakawa, T. Yamashita, and H. Fujiyoshi, “Attention branch network: Learning of attention mechanism for visual explanation,” in *2019 IEEE/CVF Conference on Computer Vision and Pattern Recognition (CVPR)*, 2019, pp. 10 697–10 706.
- [27] K. Suzuki, H. Ito, T. Yamada, K. Kase, and T. Ogata, “Deep predictive learning : Motion learning concept inspired by cognitive robotics,” 2023.
- [28] H. Ichiwara, H. Ito, K. Yamamoto, H. Mori, and T. Ogata, “Contact-rich manipulation of a flexible object based on deep predictive learning using vision and tactility,” in *2022 International Conference on Robotics and Automation (ICRA)*, 2022, pp. 5375–5381.
- [29] A. Hussein, M. M. Gaber, E. Elyan, and C. Jayne, “Imitation learning: a survey of learning methods,” *ACM computing surveys*, vol. 50, 2017.
- [30] H. Ravichandar, A. S. Polydoros, S. Chernova, and A. Billard, “Recent advances in robot learning from demonstration,” *Annual Review of Control, Robotics, and Autonomous Systems*, vol. 3, no. 1, pp. 297–330, 2020.
- [31] J. Liu, Y. Chen, Z. Dong, S. Wang, S. Calinon, M. Li, and F. Chen, “Robot cooking with stir-fry: Bimanual non-prehensile manipulation of semi-fluid objects,” *IEEE Robotics and Automation Letters*, vol. 7, no. 2, pp. 5159–5166, 2022.
- [32] H. Kim, Y. Ohmura, and Y. Kuniyoshi, “Robot peels banana with goal-conditioned dual-action deep imitation learning,” *ArXiv*, vol. abs/2203.09749, 2022.
- [33] Y. Saigusa, S. Sakaino, and T. Tsuji, “Imitation learning for non-prehensile manipulation through self-supervised learning considering motion speed,” *IEEE Access*, vol. 10, pp. 68 291–68 306, 2022.
- [34] T. Z. Zhao, V. Kumar, S. Levine, and C. Finn, “Learning fine-grained bimanual manipulation with low-cost hardware,” *Robotics: Science and Systems (RSS)*, 2023.
- [35] J. Masci, U. Meier, D. Cireşan, and J. Schmidhuber, “Stacked convolutional auto-encoders for hierarchical feature extraction,” in *Artificial Neural Networks and Machine Learning – ICANN 2011*. Springer Berlin Heidelberg, 2011, pp. 52–59.
- [36] Y. Yamashita and J. Tani, “Emergence of functional hierarchy in a multiple timescales recurrent neural network model: A humanoid robot experiment,” *PLoS Computational Biology*, vol. 4, no. 11, 2008.
- [37] Moonshot Goal3, “AI-driven Robot for Embrace and Care AIREC,” <https://airec-waseda.jp/en/toppage.en/>, [Online; accessed 23-July-2023].
- [38] Tokyo Robotics Inc., “Toward Coexistence with Robots,” <https://robotics.tokyo/>, [Online; accessed 23-July-2023].
- [39] Kinovea, <https://www.kinovea.org/>, [Online; accessed 19-August-2023].
- [40] G. Sochacki, J. Hughes, S. Hauser, and F. Iida, “Closed-loop robotic cooking of scrambled eggs with a salinity-based ‘taste’ sensor,” in *2021 IEEE/RSJ International Conference on Intelligent Robots and Systems (IROS)*, 2021, pp. 594–600.
- [41] M. Inagawa, T. Takei, and E. Imanishi, “Japanese recipe interpretation for motion process generation of cooking robot,” in *2020 IEEE/SICE International Symposium on System Integration (SII)*, 2020, pp. 1394–1399.
- [42] M. Bollini, S. Tellex, T. Thompson, N. Roy, and D. Rus, *Interpreting and Executing Recipes with a Cooking Robot*. Heidelberg: Springer International Publishing, 2013, pp. 481–495.
- [43] A. Brohan, N. Brown, J. Carbajal, Y. Chebotar, X. Chen, K. Choremanski, T. Ding, D. Driess, A. Dubey, C. Finn, P. Florence, C. Fu, M. G. Arenas, K. Gopalakrishnan, K. Han, K. Hausman, A. Herzog, J. Hsu, B. Ichter, A. Irpan, N. Joshi, R. Julian, D. Kalashnikov, Y. Kuang, I. Leal, L. Lee, T.-W. E. Lee, S. Levine, Y. Lu, H. Michalewski, I. Mordatch, K. Pertsch, K. Rao, K. Reymann, M. Ryoo, G. Salazar, P. Sanketi, P. Sermanet, J. Singh, A. Singh, R. Soricut, H. Tran, V. Vanhoucke, Q. Vuong, A. Wahid, S. Welker, P. Wohlhart, J. Wu, F. Xia, T. Xiao, P. Xu, S. Xu, T. Yu, and B. Zitkovich, “Rt-2: Vision-language-action models transfer web knowledge to robotic control,” in *arXiv preprint arXiv:2307.15818*, 2023.
- [44] J. Yi, T. A. Luong, H. Chae, M. S. Ahn, D. Noh, H. N. Tran, M. Doh, E. Auh, N. Pico, F. Yumbla, D. Hong, and H. Moon, “An online task-planning framework using mixed integer programming for multiple cooking tasks using a dual-arm robot,” *Applied Sciences*, vol. 12, no. 8, 2022.
- [45] Z. Wang, C. R. Garrett, L. P. Kaelbling, and T. Lozano-Pérez, “Learning compositional models of robot skills for task and motion planning,” in *The International Journal of Robotics Research*, vol. 40, no. 6-7, 2021, pp. 866–894.
- [46] N. Saito, J. Moura, T. Ogata, M. Y. Aoyama, S. Murata, S. Sugano, and S. Vijayakumar, “Structured motion generation with predictive learning: Proposing subgoal for long-horizon manipulation,” in *2023 IEEE International Conference on Robotics and Automation (ICRA)*, 2023, pp. 9566–9572.
- [47] S. Nair, S. Savarese, and C. Finn, “Goal-aware prediction: Learning to model what matters,” in *Proceedings of the 37th International Conference on Machine Learning*. JMLR.org, 2020.
- [48] M. S. Sakib, D. Paulius, and Y. Sun, “Approximate task tree retrieval in a knowledge network for robotic cooking,” *IEEE Robotics and Automation Letters*, vol. 7, no. 4, pp. 11 492–11 499, 2022.
- [49] Z. Wang, G. Tian, and X. Shao, “Home service robot task planning using semantic knowledge and probabilistic inference,” *Knowledge-Based Systems*, vol. 204, p. 106174, 2020.
- [50] L. Kunze and M. Beetz, “Envisioning the qualitative effects of robot manipulation actions using simulation-based projections,” *Artificial Intelligence*, vol. 247, pp. 352–380, 2017.
- [51] E. Heiden, M. Macklin, Y. Narang, D. Fox, A. Garg, and F. Ramos, “Disect: A differentiable simulation engine for autonomous robotic cutting,” *Robotics: Science and Systems (RSS)*, 2021.
- [52] D. P. Kingma and J. Ba, “Adam: A method for stochastic optimization,” *arXiv preprint arXiv:1412.6980*, 2014.